Title
Characteristics of the fourth order resonance in high intensity linear accelerators

Journal
Physics of Plasmas, 24(6)

ISSN
1070-664X

Authors
Jeon, D
Hwang, Kyung Ryun

Publication Date
2017-06-01

DOI
10.1063/1.4985685

Peer reviewed

Characteristics of the Fourth Order Resonance in High Intensity Linear Accelerators

Dong-O Jeon[1,#] and Kyung Ryun Hwang[2]

[1]Institute for Basic Science, Daejeon 34047, Republic of Korea

[2]Lawrence Berkeley Laboratory, Berkeley, CA 94720, USA

Abstract

For the $4\sigma = 360°$ space-charge resonance in high intensity linear accelerators, the emittance growth is surveyed for input Gaussian beams, as a function of the depressed phase advance per cell σ and the initial tune depression ($\sigma_o - \sigma$). For each data point, the linac lattice is designed such that the fourth order resonance dominates over the envelope instability. The data show that the maximum emittance growth takes place at $\sigma \approx 87°$ over a wide range of the tune depression (or beam current), which confirms that the relevant parameter for the emittance growth is σ and that for the bandwidth is $\sigma_o - \sigma$. An interesting four-fold phase space structure is observed that cannot be explained with the fourth order resonance terms alone. Analysis attributes this effect to a small negative sixth order detuning term as the beam is redistributed by the resonance. Analytical studies show that the tune increases monotonically for the Gaussian beam which prevents the resonance for $\sigma > 90°$. Frequency analysis indicates that the four-fold structure observed for input KV beams when $\sigma < 90°$, is not the fourth order resonance but a fourth order envelope instability because the $1/4 = 90°/360°$ component is missing in the frequency spectrum.

PACS: 29.27.Bd, 41.75.-i

Keywords: fourth order resonance; high intensity linac; space charge; envelope instability

#Corresponding author: jeond@ibs.re.kr

I. Introduction

Recently many high intensity linear accelerators have been designed and constructed like proton accelerators such as the SNS (USA) [1], J-PARC (Japan) [2], the KOMAC (Korea) [3], or heavy ion linear accelerators such as the RAON [4] or the FRIB [5]. These high intensity linacs with mega-watt class beam power have been carefully designed to minimize the beam loss of halo particles for hands-on maintenance by avoiding or minimizing the contributions of various halo formation mechanisms with the requirement of the uncontrolled beam loss less than 1 W/m.

Studies have been done in the early days related with the envelope equation [6], the particle-core model [7-10] and the envelope instability [11, 12]. In order to avoid the envelope instability, linac designers have applied the design rule to keep $\sigma_o < 90°$ [1-3] in designing high-intensity linear accelerators, where σ_o is the zero-current phase advance per cell.

Mismatch is also a well-known halo formation mechanism [13] and a proper matching between different sections of linear accelerators matters to minimize the beam loss. In order to reduce the beam loss, the idea of halo-matching was carefully studied recently [14], other than the experimental core-matching studies in the rms sense such as Ref. [15]. A fast halo formation mechanism by a non-round beam was found in the SNS linac [16] and experimentally verified [17].

Throughout this document, we call the single particle resonance simply by resonance and the coherent instability (or parametric resonance) of envelope by instability in order to avoid confusion. Even though resonances and instabilities are used in an ambiguous way in the community, instabilities should not be confused with resonances that may look similar in the phase space but each particle oscillation does not necessarily have the corresponding resonance frequency component. An example is shown in Ref. [25] of the third order instability which may be mistaken as a third-order resonance.

Studies found that space-charge resonances also can generate halos in circular and linear accelerators. It was shown that the space-charge $2\nu_x - 2\nu_y = 0$ coupling resonance induces halo in the ring [18] and later extended to linear accelerators as in Ref. [19]. The space-charge $4\sigma = 360°$ fourth order resonance in linear accelerators was found and reported to dominate over the envelope instability [20]. Here σ is the depressed phase advance per cell. In Ref. [20], much effort was taken to verify that the observed phenomenon was indeed a resonance. And the $4\sigma = 360°$ fourth order resonance was experimentally verified [21, 22]. In 2015, the space-charge $6\sigma = 720°$ sixth order resonance was found in high intensity linear accelerators [23].

It was reported that the envelope instability emerges following the fourth order resonance for high-intensity linear accelerators with a constant σ_o lattice [24], which seemed to suggest that the envelope instability dominates over the fourth order resonance in the long run. But a later study clarified that the fourth order resonance dominates over the envelope instability when σ is kept constant along the linac, and

that the envelope instability emerges from the mismatch by the fourth order resonance when σ_o is kept constant along the linac [25].

This paper reports the characteristics of the $4\sigma = 360°$ fourth order resonance along with the fourth order envelope instability in high intensity linear accelerators: 1) the emittance growth as a function of the initial tune depression and the depressed phase advance per cell σ, 2) the sixth order detuning effect induced by the beam redistribution due to the fourth order resonance, 3) analytical study of the detuning of the Gaussian beam, and 4) the fourth order envelope instability of the KV beam.

II. Characteristics of fourth order resonance

Numerical simulations are performed with initially well-matched Gaussian beams with 20,000 to 100,000 macro-particles using the PARMILA code with a 3D Particle-In-Cell space-charge routine [26]. 5 ~ 40 emA $_{40}Ar^{+10}$ beams with initial normalized rms emittance $\varepsilon_x = \varepsilon_y = 0.115$ [mm mrad], $\varepsilon_z = 0.120$ [mm mrad] are used for simulations. The beam has the initial energy of 5 MeV/u and is accelerated to $\beta = 0.24$ or higher. The coupling between the transverse and longitudinal planes is minimal because the depressed longitudinal phase advance is about 10°, well separated from the depressed transverse phase advance under consideration. A linac with an FOFODODO transverse focusing lattice is used for simulations. The acceleration voltage is applied in the drifts that are denoted as "O" of the FOFODODO.

The emittance growth factor ($= \varepsilon_{final} / \varepsilon_{initial}$) is plotted in Fig. 1 as a function of the initial tune depression ($\sigma_o - \sigma$) and depressed phase advance per cell σ. The tune depression ($\sigma_o - \sigma$) in Fig. 1 is the initial tune depression and tends to decrease as the

beam accelerates. It should be noted that the emittance growth is solely due to the fourth order resonance. The linac lattice is adjusted such that σ is kept constant throughout the linac and only the fourth order resonance is manifested and the envelope instability suppressed for any data points in Fig. 1, as reported in Ref. [25].

Over a wide range of the initial tune depression (or beam current), the maximum emittance growth happens at $\sigma \approx 87°$ and no resonance effect is observed for $\sigma > 90°$ regardless of the tune depression. This shows that, in case of the single particle resonance, the relevant parameter for maximum emittance growth is σ and that for bandwidth is $\sigma_o - \sigma$. It should be noted that there is no resonance, nor associated emittance growth for $\sigma > 90°$. The reason is explained in the later section of the analytical analysis.

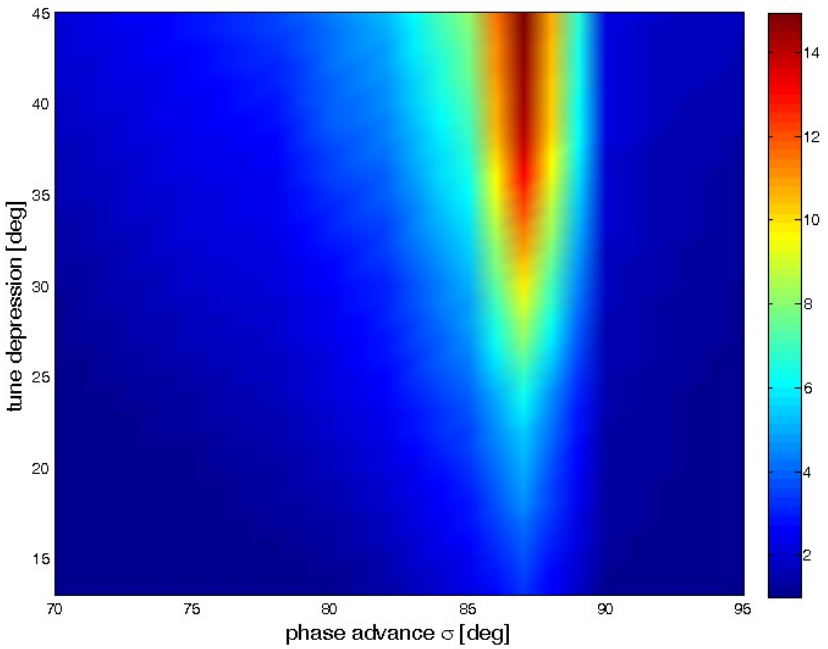

FIG. 1. 2D plot of emittance growth factor ($= \varepsilon_{final} / \varepsilon_{initial}$) by the $4\sigma = 360°$ space-charge resonance as a function of the initial tune depression ($\sigma_o - \sigma$) and depressed phase advance per cell σ. Regardless of the tune depression (or beam current), maximum

emittance growth happens at $\sigma \approx 87°$ just below 90°. For each data point, the linac lattice is designed such that σ is kept constant along the linac to ensure that only the fourth order resonance is manifested and the envelope instability suppressed. And there is no resonance, nor associated emittance growth for $\sigma > 90°$.

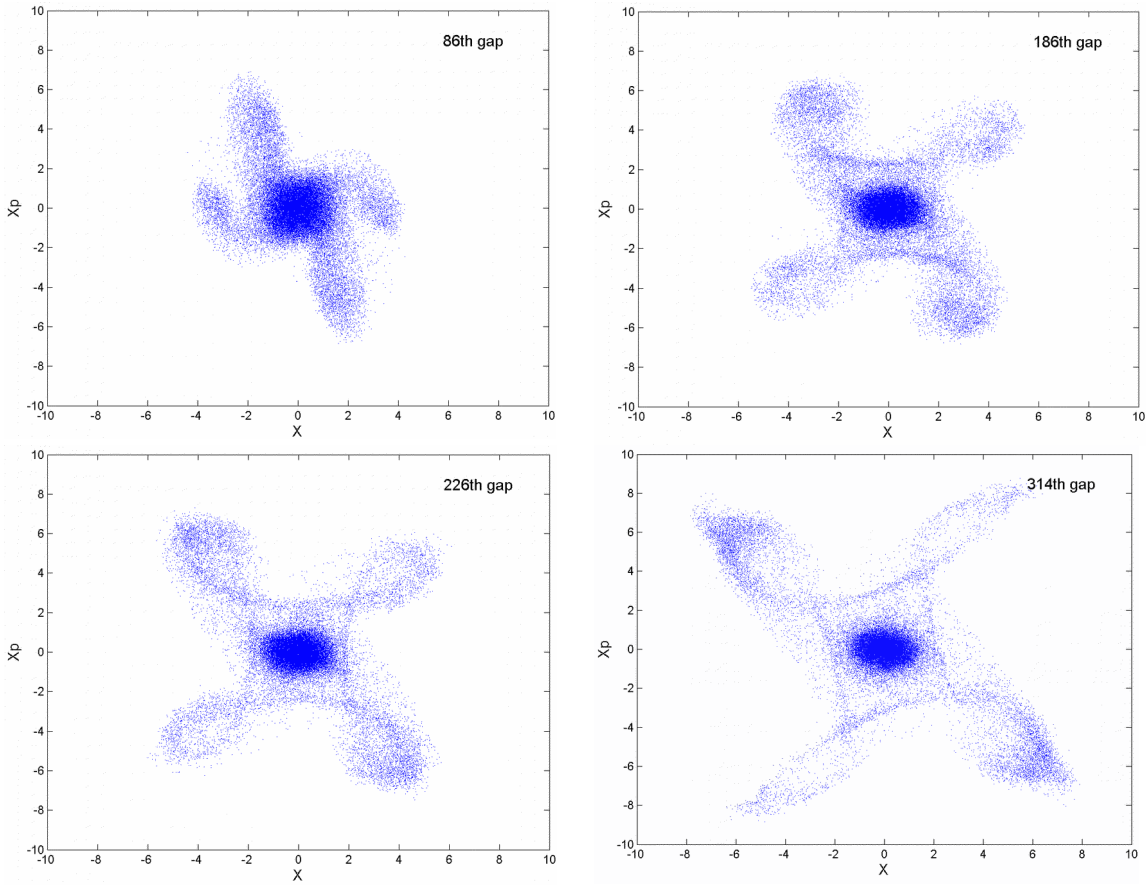

FIG. 2. Plots of the beam distribution evolution in the normalized X phase space under the $4\sigma = 360°$ space-charge resonance along the linac (increasing accelerating RF gap numbers). The multiparticle simulation is made for a linac lattice with a constant depressed phase advance per cell $\sigma = 87°$ throughout the linac and for an initially well-matched Gaussian 30-emA $_{40}Ar^{+10}$ beam. Only the fourth order resonance is manifested and the envelope instability suppressed. 30-emA beam current corresponds to the initial

tune depression of 39° in Fig. 1. Normalization of coordinates is made with respect to the halo rather than the core.

Because the fourth order $4\sigma = 360°$ resonance dominates, the system can be described as a Hamiltonian. However, the phase space structure in Fig. 2 cannot be explained with the fourth order resonance terms alone in the Hamiltonian. Analysis indicates that this particular four-fold structure is attributed to a small negative sixth-order I^3 detuning term. From the locations of the stable and unstable fixed points in phase space, the corresponding Hamiltonians are obtained at two locations of the linac as Eq. (1) the 226th RF gap and as Eq. (2) at the 314th RF gap:

, (1)

, (2)

where $\nu = \sigma/360°$. Here I, ϕ are the action, angle variables of the Hamiltonian. In the Hamiltonian, only even order terms such as etc are included because the accelerators have x(y) symmetry and the initial beam distributions are symmetric. The Hamiltonian changes from gap to gap as the beam is accelerated in the linac and the accelerating structure changes smoothly.

Figure 3 displays the phase space structure of the Hamiltonian in Eq. (1) in the top plot and that of Eq. (2) in the bottom plot. The agreement between Fig. 2 and Fig. 3 shows that the Hamiltonians in Eq. (1) and (2) describe well the phase space structure in Fig. 2 such as the fixed points and separatrices. This supports our confidence in that the system is described by the resonance Hamiltonian and the fourth order resonance domination over the fourth order envelope instability. In addition, this agreement allows

us to interpret the occurrence of maximum emittance growth $\sigma = 87°$ regardless of the beam intensity, in terms of single particle Hamiltonian.

The effect of the sixth order term becomes noticeable, as the beam is redistributed by the fourth order resonance. It is shown in Fig. 4 that a redistribution of the beam by the fourth order resonance alters the space charge field (denoted as Ex), as the particular four-fold structure emerges. And the beam is no longer Gaussian.

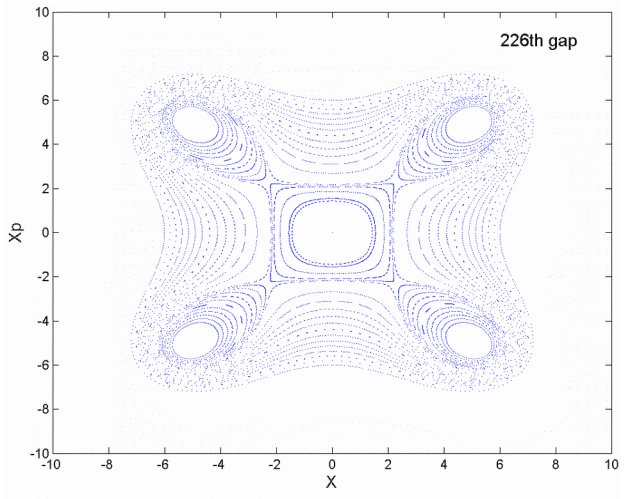

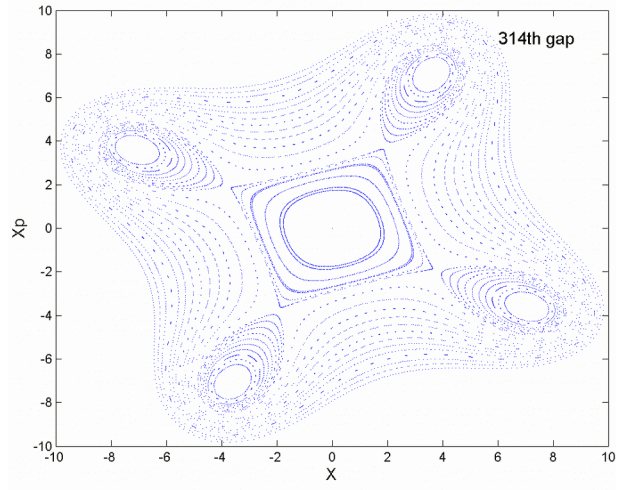

FIG. 3. Phase space plots showing the fourth order resonance structure with the sixth order detuning term. The top plot shows the structure of Eq. (1) reproducing the phase space structure at the 226th RF gap in Fig. 2 and the bottom plot the structure of Eq. (2)

reproducing the phase space structure at the 314th RF gap in Fig. 2. This shows that the phenomenon is dominated and governed by the single particle Hamiltonian. X and Xp are normalized coordinates and .

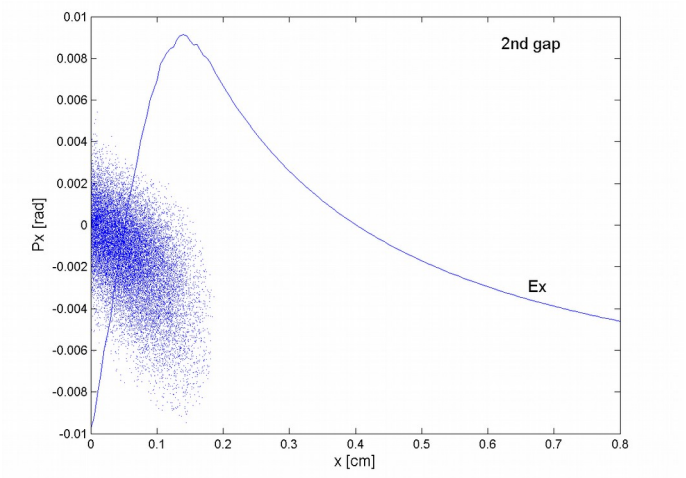

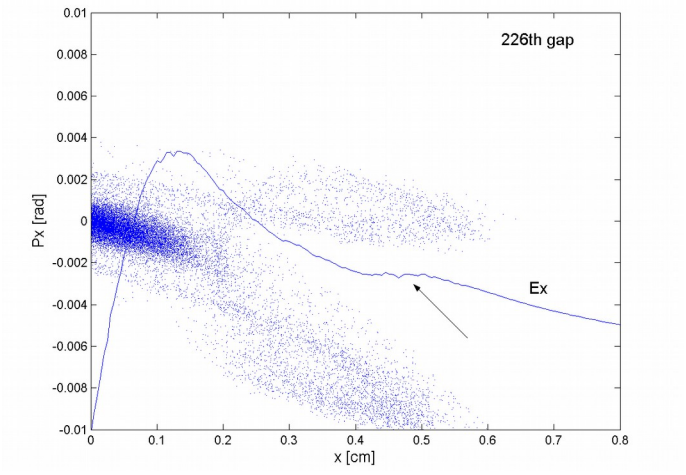

FIG. 4. Plots of beam distribution in phase space and its corresponding space charge electric field superimposed at the 2nd RF gap (the top plot) and at the 226th RF gap (the bottom plot) of the linac. Redistribution of the beam particles by the fourth order resonance changes the space charge field and the particular four-fold structure emerges.

The input beam is 3D Gaussian and it is worthy to study its higher order detuning effects to explain why there is no resonance for $\sigma > 90°$ and to explain the maximum emittance growth at $\sigma = 87°$. We resort to the available analytical expression of the space charge Hamiltonian for the 2D Gaussian beam [27, 25], which is given by

(3)

(4)

where s is the longitudinal coordinate on reference orbit, $K_x(s)$ and $K_y(s)$ are focusing field strength, $\sigma_x^2=\beta_x\varepsilon_x$ and $\sigma_y^2=\beta_y\varepsilon_y$ are the beam sizes, (I_x, ϕ_x) action, angle variables, , and with the classical proton radius .

Detuning terms correspond to the zero harmonic of the potential, i.e.:

(5)

Then, the incoherent tune shift becomes

(6)

where J_i is the i-th order Bessel function, and and , and $\nu = \sigma/360°$.

Expanding in order of , integrating over t , the is expressed as

(7)

Then the incoherent tune shift becomes

(8)

and the Laslett tune shift .

Figure 5 illustrates dependence of the detuning on particle oscillation amplitude using the Eq. (8). The phase advance or tune of individual particles of the exact expression and a few truncated Taylor expansions are shown as a function of action I_x. Monotonic increase of the exact phase advance of the Gaussian beam explains why there is no fourth order resonance when $\sigma_o + \Delta\sigma_{Laslett} > 90°$ (as reported in [20]), because the phase advance curve of the exact expression does not cross the 90° line. It should be noted that this is the result of 2D Gaussian beam.

Since the majority of particles are at the beam core, there are more particles that participate in resonance when σ is slightly below 90°. And when more particles are on resonance, larger emittance growth is expected. Since the core particles have small oscillation amplitude, this also explains why higher order resonances appears to be weak and numerical study at $6\sigma = 360°$ resonance showed little emittance growth [23].

For Gaussian beams, truncation of the detuning terms at a finite order can lead to an unphysical system, as shown by the cyan curve that is truncated at the term. In this case, a four-fold resonance structure is observed above 90° because the phase advance curve crosses the 90° line.

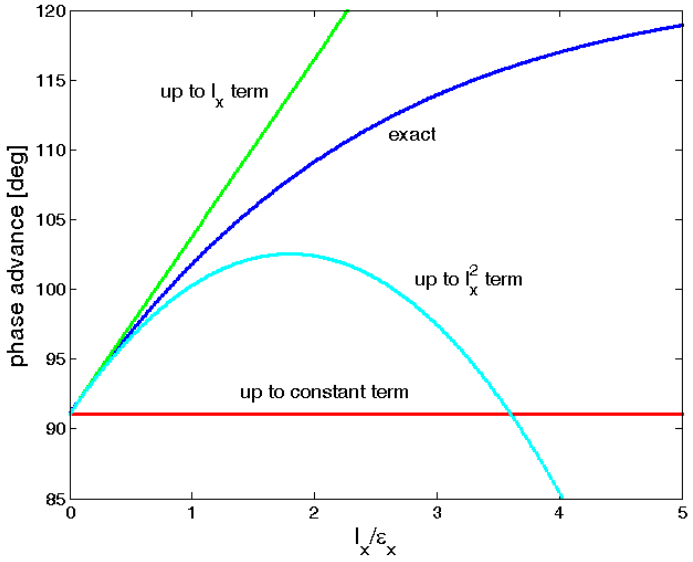

FIG. 5. Plot of the phase advance as a function of particle action I_x for $\sigma_o + \Delta\sigma_{Laslett} = 91°$ case with . The ensemble average is $\sigma = 93°$. Note that the exact phase advance of the 2D Gaussian beam diverges from those of the truncated Taylor expansions. Monotonic increase of the exact phase advance of the Gaussian beam explains why there is no fourth order resonance when $\sigma_o + \Delta\sigma_{Laslett} > 90°$ because the phase advance curve does not cross the 90° line.

III. Fourth order envelope instability

Around 90° phase advance, there are three mechanisms: the $4\sigma = 360°$ fourth order resonance [20], the second envelope instability ($2\sigma_o - \Delta\sigma_{2,coh} = 180°$) and the fourth order envelope instability ($4\sigma_o - \Delta\sigma_{4,coh} = 360°$) [11]. For realistic beams, the fourth order resonance dominates over the fourth order instability and the envelope instability is either suppressed or manifested, depending on σ, σ_o of the lattice [23].

It is known that numerically generated KV beams also produce a four-fold structure [29] like realistic beams such as Gaussian and waterbag beams. Simulations are done for a lattice with a constant $\sigma_o = 106°$ ($\sigma = 85°$ initially and reaches 94°) and for $_{40}Ar^{+10}$ 10-emA KV beam. In order to check whether this is the fourth order resonance or the fourth order envelope instability, an FFT analysis is performed on the rms beam size. In Fig. 6, the resultant frequency spectrum does not show the component at 1/4 = 90°/360°, indicating that this is the fourth order envelope instability not the fourth order resonance. However, the spectral component at 1/4 = 90°/360° is sometimes observed depending on σ, σ_o of the lattice and the numerical noise of the KV distribution. It should be noted that the beam is no longer a KV beam, as the four-fold structure develops. Also the spectrum is very sensitive to the generated initial beam distributions. The spectrum changes as the simulation is repeated.

It is observed that the four-fold structure does not develop well for $\sigma > 90°$. For a KV beam, only a slight hint of the four-fold structure is observed for the lattice with constant $\sigma \approx 92°$ (initial $\sigma_o = 114°$). Simulations are done also for a lattice with constant $\sigma_o = 120°$. The initial σ is controlled by varying the beam current. When the initial σ is above 90°, only a slight hint of the four-fold structure is observed, whereas the four-fold structure is observed when the initial σ is below 90°.

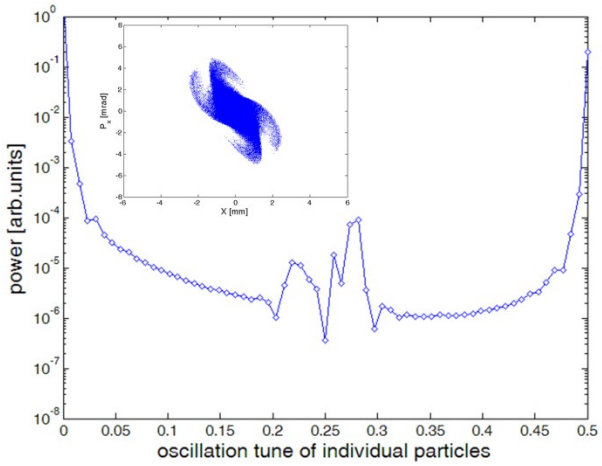

FIG. 6. Plot of the FFT power spectrum of the rms beam size for input KV beam. The FFT frequency spectrum does not show the component at 1/4 = 90°/360° suggesting that this is the fourth order envelope instability, not the fourth order resonance. However, the spectral component at 1/4 = 90°/360° is sometimes observed depending on σ, σ_o of the lattice and the numerical noise of the beam distribution. Simulations are done for a lattice with constant σ_o = 106° (initially σ = 85° and reaches 94°) and for a $_{40}Ar^{+10}$ 10-emA KV beam. However, the spectral component at 1/4 = 90°/360° is sometimes observed depending on σ, σ_o of the lattice and the numerical noise of the KV distribution.

IV. Summary

The emittance growth by the 4σ = 360° space-charge resonance is surveyed, as a function of the depressed phase advance per cell σ and the initial tune depression ($\sigma_o - \sigma$). For each data point, the linac lattice is designed such that the fourth order resonance dominates over the envelope instability. The data show that the maximum emittance growth takes place at $\sigma \approx 87°$ regardless of the tune depression (or beam

current), which confirms that the relevant parameter for the emittance growth is σ and the relevant parameter for the bandwidth is $\sigma_o - \sigma$.

An interesting four-fold phase space structure is observed and the analysis attributes this effect to a small negative sixth order detuning term generated as the beam is redistributed by the resonance. Analytical studies show that the tune increases monotonically for the Gaussian beam, which prevents the resonance for $\sigma > 90°$. Frequency analysis indicates that the four-fold structure, observed for input KV beams when $\sigma < 90°$, is not the fourth order resonance but a fourth order envelope instability because the $1/4 = 90°/360°$ component is missing in the frequency spectrum. The four-fold structure does not develop well for $\sigma > 90°$.

Acknowledgements

This work was supported by the Rare Isotope Science Project of the Institute for Basic Science funded by the Ministry of Science, ICT and Future Planning (MSIP) and the National Research Foundation (NRF) of the Republic of Korea under Contract 2013M7A1A1075764. This is also supported by U.S. Department of Energy under Contract No. DE-AC02-05CH11231.

References

[1] S. Henderson, W. Abraham, A. Aleksandrov, C. Allen, J. Alonso, D. Anderson, D. Arenius, T. Arthur, S. Assadi, J. Ayers et al., Nucl. Instr. Meth. A **763** (2014) 610; J.

Stovall, J.H. Billen, S. Nath, H. Takeda, L.M. Young, D. Jeon, Proc. of 2001 Part. Accl. Conf., Chicago, USA, p. 446.

[2] Y. Yamazaki, Proc. of 2003 Part. Accl. Conf., Portland, USA, p. 576.

[3] Byung-Ho Choi, Proc. of 2004 Asian Part. Accl. Conf., Gyeongju, Korea (IEEE, New York, 2004), p. 231.

[4] D. Jeon, I.S. Hong, H.J. Kim, J.W. Kim, R.M. Bodenstein, H.J. Cha, S.J. Choi, S. Choi, O.R. Choi, H. Do et al., J. Korean Phys. Soc. **65**, 1010 (2014). DOI: 10.3938/jkps.65.1010; Ji-Gwang Hwang, Eun-San Kim, Hye-Jin Kim, Hyojae Jang, Hyung-Jin Kim, Dong-O Jeon, IEEE Trans. Nucl. Sci. **63**, 992 (2016).

[5] J. Wei, D. Arenius, E. Bernard, N. Bultman, F. Casagrande, S. Chouhan, C. Compton, K. Davidson, A. Facco, V. Ganni et al., Proc. of 2012 Linear Accl. Conf., Tel-Aviv, Israel (IEEE, New York, 2012), p. 417.

[6] F.J. Sacherer, IEEE Trans. Nucl. Sci. **18**, 1105 (1971); P.M. Lapostolle, *ibid*. **18**, 1101 (1971).

[7] J.S. O'Connell, T.P. Wangler, R.S. Mills, and K.R. Crandall, Proc. of 1993 Part. Accl. Conf., Washington D.C., USA (IEEE, New York, 1993), p. 3657.

[8] Jean-Michel Lagniel, Nucl. Instr. and Meth. A **345** (1994) 46; R.L. Gluckstern, Phys. Rev. Lett. **73**, 1247 (1994).

[9] Jean-Michel Lagniel and David Libault, Proc. of 1995 Part. Accl. Conf., Dallas, USA (IEEE, New York, 1995), p. 446.

[10] T.P. Wangler, K.R. Crandall, R. Ryne, and T.S. Wang, Phys. Rev. ST Accel. Beams **1**, 084201 (1998).

[11] I. Hofmann, L.J. Laslett, L. Smith, and I. Harber, Part. Accel. **13**, 145 (1983).

[12] J. Struckmeier and M. Reiser, Part. Accel. **14**, 227 (1984).

[13] J. D. Lawson, *The Physics of Charged Particle Beams*, 2nd ed., Oxford University Press, New York, 1988.

[14] P.A.P. Nghiem, N. Chauvin, M. Comunian, O. Delferriere, R. Duperrier, A. Mosnier, C. Oliver, D. Uriot, Nucl. Instr. Meth. A **654** (2011) 63; P.A.P. Nghiem, N. Chauvin, S. Simeoni, Jr., D. Uriot, App. Phys. Lett. **104**, 074109 (2014).

[15] K.R. Crandall, Proc. of 1972 Proton Linear Accelerator Conference, Los Alamos, USA, p. 51; D. Jeon, C.M. Chu, J. Stovall, S. Assadi, Nucl. Instr. Meth. A **607** (2009) 517.

[16] D. Jeon, J. Stovall, A. Aleksandrov, J. Wei, J. Staples, R. Keller, L. Young, H. Takeda, S. Nath, Phys. Rev. ST Accel. Beams **5**, 094201 (2002).

[17] Dong-O Jeon, Phys. Rev. ST Accel. Beams **16**, 040103 (2013).

[18] D. Jeon, J.A. Holmes, V.V. Danilov, J.D. Galambos, D.K. Olsen, Phys. Rev. E **60**, 7479 (1999); E. Metral et al, Proc. of 2004 European Part. Accel. Conf., Lucerne, Switzerland, p. 1894; I. Hofmann, G. Franchetti, Phys. Rev. ST Accel. Beams **9**, 054202 (2006).

[19] G. Franchetti, I. Hofmann, D. Jeon, Phys. Rev. Lett. **88**, 254802 (2002); I. Hofmann, G. Franchetti, O. Boine-Frankenheim, J. Qiang, R. Ryne, D. Jeon, J. Wei, Proc. of 2001 Part. Accel. Conf., Chicago, USA, p. 2902.

[20] D. Jeon, L. Groening, G. Franchetti, Phys. Rev. ST Accel. Beams **12**, 054204 (2009).

[21] L. Groening, W. Barth, W. Bayer, G. Clemente, L. Dahl, P. Forck, P. Gerhard, I. Hofmann, M.S. Kaiser, M. Maier, S. Mickat, T. Milosic, D. Jeon, D. Uriot, Phys. Rev. Lett. **102**, 234801 (2009).

[22] Dong-O Jeon, Phys. Rev. Accel. Beams **19**, 010101 (2016).

[23] Dong-O Jeon, Kyung Ryun Hwang, Ji-Ho Jang, Hyunchang Jin, Hyojae Jang, Phys. Rev. Lett. **114**, 184802 (2015).

[24] I. Hofmann and O. Boine-Frankenheim, Phys. Rev. Lett. **115**, 204802 (2015).

[25] D. Jeon, J.-H. Jang and H. Jin, Nucl. Instr. Meth. A **832** (2016) 43.

[26] H. Takeda and J. Stovall, Proc. of 1995 Part. Accl. Conf., Dallas, USA, p.2364.

[27] X. Pang, F. Wang, X. Wang, S.Y. Lee, Proc. of Hadron Beam 2008, Nashville, USA, p. 118.

[28] J. Qiang, R. Ryne, S. Habib, V. Decyk, J. Comp. Phys. **163**, 434 (2000).

[29] I. Harber and A.W. Maschke, Phys. Rev. Lett. **42**, 1479 (1979).